JOURNAL OF GEOPHYSICAL RESEARCH, VOL. 103, NO. B12, PAGES 30,101–30,115, DECEMBER 10, 1998

Location of the southern edge of the Gorda slab and evidence for an adjacent asthenospheric window: Results from seismic profiling and gravity

Bruce C. Beaudoin, John A. Hole,[1] and Simon L. Klemperer
Department of Geophysics, Stanford University, Stanford, California

Anne M. Tréhu
College of Ocean and Atmospheric Sciences, Oregon State University, Corvallis

Abstract. As the Mendocino Triple Junction migrates northward along the California margin it is widely presumed to leave a "slab-free" or "asthenospheric" window in its wake. A 250-km-long south-north seismic refraction-reflection profile crossing the transition from transform to subduction regimes allows us to compare and contrast crust and upper mantle of the North American margin before and after it is modified by passage of the Mendocino Triple Junction. From the seismic data we have determined that (1) the crust is laterally homogeneous in velocity to a depth of 20 km (interpreted by us as Franciscan complex), (2) below 20 km depth the crust is characterized by velocities of $\geq$7.0 km/s for the southern half of the profile and by velocities of $\leq$7.0 km/s for the northern half, (3) regions of high reflectivity in the crust occur below ~20 km depth throughout the profile, and (4) the North American crust is thickest (~35 km) in the center of the profile and thins to ~25 km at either end. From the gravity data we have determined that (1) asthenospheric densities (3.2 g/cm^3) occur subjacent to the North American crust in the center of the profile, and (2) a wedge of lithospheric mantle density material ($\geq$3.2 g/cm^3) is required on the southern end of the profile. We interpret these combined results to indicate that our profile crosses the southern edge of the Gorda plate and that directly adjacent to this edge is an asthenospheric window with overlying mafic rocks in the crust. These mafic rocks and a reforming lithospheric mantle increase in thickness southward.

1. Introduction

Northern California tectonics are governed by the interactions of the Pacific, Gorda, and North American plates. (We use the term Gorda plate while recognizing that recent work suggests that Gorda deformation zone may be more appropriate [*Wilson*, 1989].) The three plates come together at the Mendocino Triple Junction (MTJ) (Figure 1), a transform-transform-trench triple junction that was initiated at 25–29 Ma by the collision of a Pacific spreading center with the North American continent [*Atwater*, 1970]. As the Juan de Fuca–Pacific plate boundary migrates northward relative to North America, subduction along the Cascadia subduction zone is replaced by the transform boundary of the San Andreas fault system (Figure 1). Today, the MTJ is defined by a broad onshore region near Cape Mendocino [*Clarke*, 1992] and provides a unique laboratory to study plate interactions at a triple junction. The transition from a subduction regime to a transform regime has long been recognized from geological studies, and its subsurface manifestations have been recognized from upper mantle velocity tomography and potential field studies. How this transition is accommodated on a detailed crustal and lithospheric scale, however, is only now being examined with seismic refraction and reflection techniques.

In the currently most popular model for evolution of the MTJ, first formulated in a rigid-plate model by *Dickinson and Snyder* [1979], an important consequence of MTJ migration is that the North American plate slides off the Gorda plate, leaving in its wake a void that is filled by upwelling asthenosphere, referred to as the slabless window or slab gap [*Dickinson and Snyder*, 1979; *Severinghaus and Atwater*, 1990]. Supporting evidence for a slabless window exists from heat flow data [*Lachenbruch and Sass*, 1980], gravity and magnetic data [*Griscom and Jachens*, 1989; *Jachens and Griscom*, 1983], teleseismic *P* wave delay studies [*Benz et al.*, 1992; *Verdonck and Zandt*, 1994; *Zandt*, 1981; *Zandt and Furlong*, 1982], shear wave velocities [*Levander and Kovach*, 1990], and changes in volcanism [*Dickinson and Snyder*, 1979; *Fox et al.*, 1985; *Furlong*, 1984; *Johnson and O'Neil*, 1984; *Zandt and Furlong*, 1982]. These studies further suggest that (1) the observed upper mantle low-velocity zone is smaller and displaced to the east compared to that predicted by rigid-plate models; (2) the Gorda slab is fragmenting along its southern edge; (3) arc volcanism is being replaced by bimodal volcanism that exhibits a northward decrease in age; and (4) the eastern boundary of the Pacific plate has migrated eastward through a series of jumps of the Mendocino Triple Junction. Some of these complexities may be explained by introducing more complex rheologies and thermal distributions into the simple rigid-plate model of Dickinson and Snyder. For example, thermomechanical modeling

[1]Now at Department of Geological Sciences, Virginia Polytechnic Institute and State University, Blacksburg.

Paper number 98JB02231.
0148-0227/98/98JB-02231$09.00

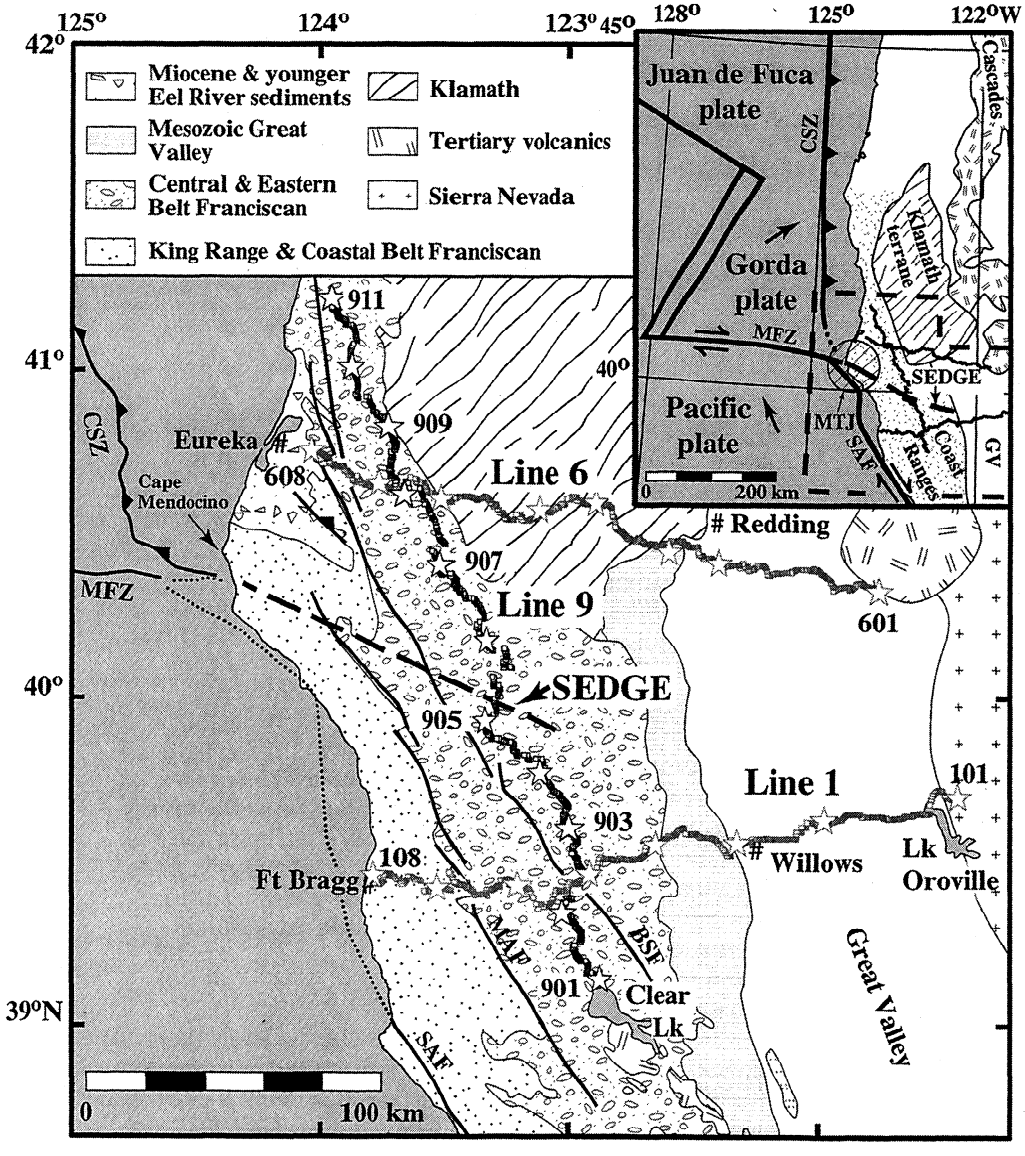

Figure 1. Generalized geologic map of northern California. Squares, instrument locations, which commonly overlap to form solid lines; stars, shot point locations; BSF, Bartlett Springs fault; CSZ, Cascadia subduction zone; MAF, Maacama fault; MFZ, Mendocino fracture zone; SAF, San Andreas fault; SEDGE, southern edge of the Gorda slab as determined from this study. Inset shows tectonic setting of the Mendocino Triple Junction Seismic Experiment. Wiggly lines, seismic profiles; large arrows, plate motion relative to fixed North America; MTJ, Mendocino Triple Junction; GV, Great Valley.

suggests that the boundary at depth between the Pacific and North American plates should step inboard with time as the slabless window cools and new material is accreted to the edge of the Pacific plate [*Furlong et al.*, 1989]; recent results suggest that such a process may be occurring in the San Francisco Bay region [*Brocher et al.*, 1994]. Alternatively, the slabless window model may be fundamentally incorrect for northern California. *Bohannon and Parsons* [1995] recently questioned the long-standing paradigm of a slabless window for the MTJ region. On the basis of analysis of plate motions and geometries, Bohannon and Parsons suggest that coastal California should be underlain by a stalled slab rather than a slabless gap; in their model a slabless window may exist but would be much farther inland.

Our study focuses on the transition from subduction to transform tectonics by analyzing a SE-NW trending wide-angle reflection profile herein referred to as line 9 (Figure 1). These data were part of the first phase of the Mendocino Triple Junction Seismic Experiment (MTJSE) collected in 1993 [*Beaudoin et al.*, 1996; *Godfrey et al.*, 1995; *Tréhu et al.*, 1995]. During this 1993 field season we collected 650 km of onshore seismic refraction data: line 1 sampling the transform regime; line 6 sampling the subduction regime; and line 9 sampling the transition from transform to subduction regimes (Figure 1). The MTJSE is a multiyear, multiinstitutional effort to study the lithospheric response to MTJ passage by comparing and contrasting the subduction regime to the transform regime.

2. Tectonic and Geologic Setting

2.1. Plate Geometry and Cascadia Seismicity

As the Gorda-Pacific plate boundary migrates northward relative to North America, subduction along the Cascadia sub-

duction zone is replaced by the transform boundary of the San Andreas fault system (Figure 1). North of the MTJ, the tectonics are governed by the subduction of young (~5 Ma) Gorda plate obliquely beneath North American plate along the Cascadia subduction zone. South of the MTJ the tectonics are governed by the transform boundary between the Pacific and North American plates, the San Andreas fault system. Offshore, the boundary between the Pacific and Gorda plates defines the Mendocino fracture zone which juxtaposes the young Gorda plate with the older (~26 Ma) Pacific plate. Kinematic modeling of northward convergence of the Pacific plate with the Gorda plate indicates that the southeastern portion of the Gorda plate, nearest the MTJ, is undergoing the greatest amount of compressional strain in a north-south direction [*Wilson*, 1986], further complicating our understanding of the MTJ region.

The MTJ region has experienced over 60 earthquakes of $M_S \geq 5.5$ since 1853 [*Oppenheimer et al.*, 1993]. Recent analysis of the physical characteristics of the Cascadia subduction zone and seismicity of the Juan de Fuca–Gorda plate and surface deformation indicate the Cascadia subduction zone may be a well-coupled or fully locked system with potential for large ($M_S \geq 8$) subduction zone earthquakes [*Carver and Burke*, 1989; *Clarke and Carver*, 1992; *Heaton and Hartzell*, 1987]. In the subduction regime, earthquakes are common to depths of 40 km and largely result from internal deformation of the subducting Gorda slab and slip along the Mendocino fracture zone [*Castillo and Ellsworth*, 1993]. In contrast, in the transform regime, earthquakes are normally shallower than ~15 km and reflect the right-lateral motion between Pacific and North American plates [*Castillo and Ellsworth*, 1993].

2.2. Geologic Overview

Northern coastal California records a history of subduction and accretion that has been active since at least the Early Cretaceous [*Dickinson*, 1981]. The overriding North American plate in the MTJ region consists of accretionary wedges of the Mesozoic-Cenozoic Franciscan complex [e.g., *Blake et al.*, 1985] overlain by the Eel River Basin, a Cenozoic forearc basin [*Clarke*, 1992] (Figure 1). The Franciscan complex increases in age and metamorphic grade inboard and is largely composed of metasedimentary rocks. It has been divided into three belts: the Coastal belt, consisting predominantly of a Tertiary accretionary complex; the Central belt, a tectonic mélange of Early Jurassic to Tertiary(?) age; and the Eastern belt, Jurassic to Cretaceous blueschist-facies rocks (Figure 1) [*Blake et al.*, 1985]. Onshore, the Eel River Basin consists of up to 4 km of Miocene and younger sedimentary rocks that lie unconformably on Coastal and Central belt Franciscan complex [*Clarke*, 1992]. Line 9 is roughly parallel to the geologic strike of the region and is therefore approximately in the same Franciscan subterrane throughout its length (Figure 1).

North of the present-day MTJ, the Franciscan belts along the Cascadia subduction zone are overlain by the Klamath terrane, composed of arc-related rocks of Paleozoic to Late Jurassic age [*Harper*, 1980]. Accretion of the Klamath terrane to the North American margin occurred during the Late Jurassic [*Blake and Jayko*, 1986]. The contact between the Klamath terrane and the Eastern belt Franciscan is thought to be an east dipping thrust fault [cf. *Beaudoin et al.*, 1996; *Tréhu et al.*, 1995]. South of the present MTJ and Klamath belt, continentward accretion of the Franciscan was limited by crustal-scale wedging beneath the older Great Valley forearc basin and its ophiolitic basement [*Godfrey et al.*, 1997].

3. Modeling: Technique, Results, and Errors

The model presented herein is the result of inverse modeling of travel times of both refracted and reflected arrivals [*Hole*, 1992; *Hole and Zelt*, 1995] (Plate 1). The model presented has an overall absolute value rms fit of 82 ms to first arrivals. In addition to travel time modeling, we have also incorporated a depth-migrated single-fold image of the precritical reflections from offsets of ≤30 km, and gravity modeling, to constrain possible tectonic models.

3.1. Velocity and Interface Modeling

The velocity modeling was carried out in two stages. First, travel times for *Pg*, defined as the diving wave in the crust, were picked, and these travel times were inverted for velocity. The final inversion model has a 1 km square grid velocity parameterization and a 20-km-horizontal × 4-km-vertical smoothing operator applied. The Franciscan complex has few coherent seismic reflectors. Hence we are unconcerned with midcrustal events in this data set since they are isolated features (observable on fewer than three shot gathers; for a detailed discussion of the effect the Franciscan complex has on the wave field, see *Lendl et al.* [1997]). Once the crustal velocity structure is established, we can infer first-order discontinuities from the presence of steep gradients, although the method is not designed to have explicit velocity discontinuities. Our inversion method does allow the placement of a reflector within the model by "floating" the interface over the velocity field to minimize reflection travel time residuals without updating the model velocities. Hence we introduced interfaces for the basal crustal and Moho reflections based on the wide-angle reflections along the profile. The modeled locations of these reflectors coincide with many of the high-amplitude reflections on the depth-migrated single-fold image (see below).

3.1.1. The subduction regime (model coordinates ~110–250 km). The Franciscan complex between shot points 906 and 911 exhibits the largest amount of lateral variation along the profile (Plate 1). Lateral variations in velocity as large as 0.5 km/s in 25 km are modeled from refracted arrivals in the upper 10 km beneath shot points 907, 908, and 909. There is no evidence of higher-velocity Klamath rocks beneath these shot points [*Beaudoin et al.*, 1996; *Tréhu et al.*, 1995]. Beneath 10 km depth the velocity field is laterally uniform to 20 km depth (the 6.5 km/s contour). However, it is likely that variations of the scale observed in the upper 10 km are present but not resolved [*Lendl et al.*, 1997]. Refracted arrivals sampling deeper in the model define a gently SE dipping velocity boundary to ~35 km depth. Mantle diving rays, arrivals with apparent velocities ≥7.6 km/s, are observed from shot points 903, 905, 906, 909, and 911 (Figure 2). Lower crustal and mantle ray coverage from these arrivals is limited to a region between coordinates ~95 km and ~215 km.

Reflections from the lower crust and Moho are observed in both the wide-angle (Figure 2) and depth-migrated single-fold data (Figure 3). The depth-migrated single-fold image defines a segment of an intracrustal interface with an apparent dip of ~10° SE. Wide-angle reflections from shot points 906 and 907 (Figure 2) are modeled as an interface that is coincident with the depth-migrated single-fold image at a depth of 25–29 km between model coordinates 125 and 150. The inverse method

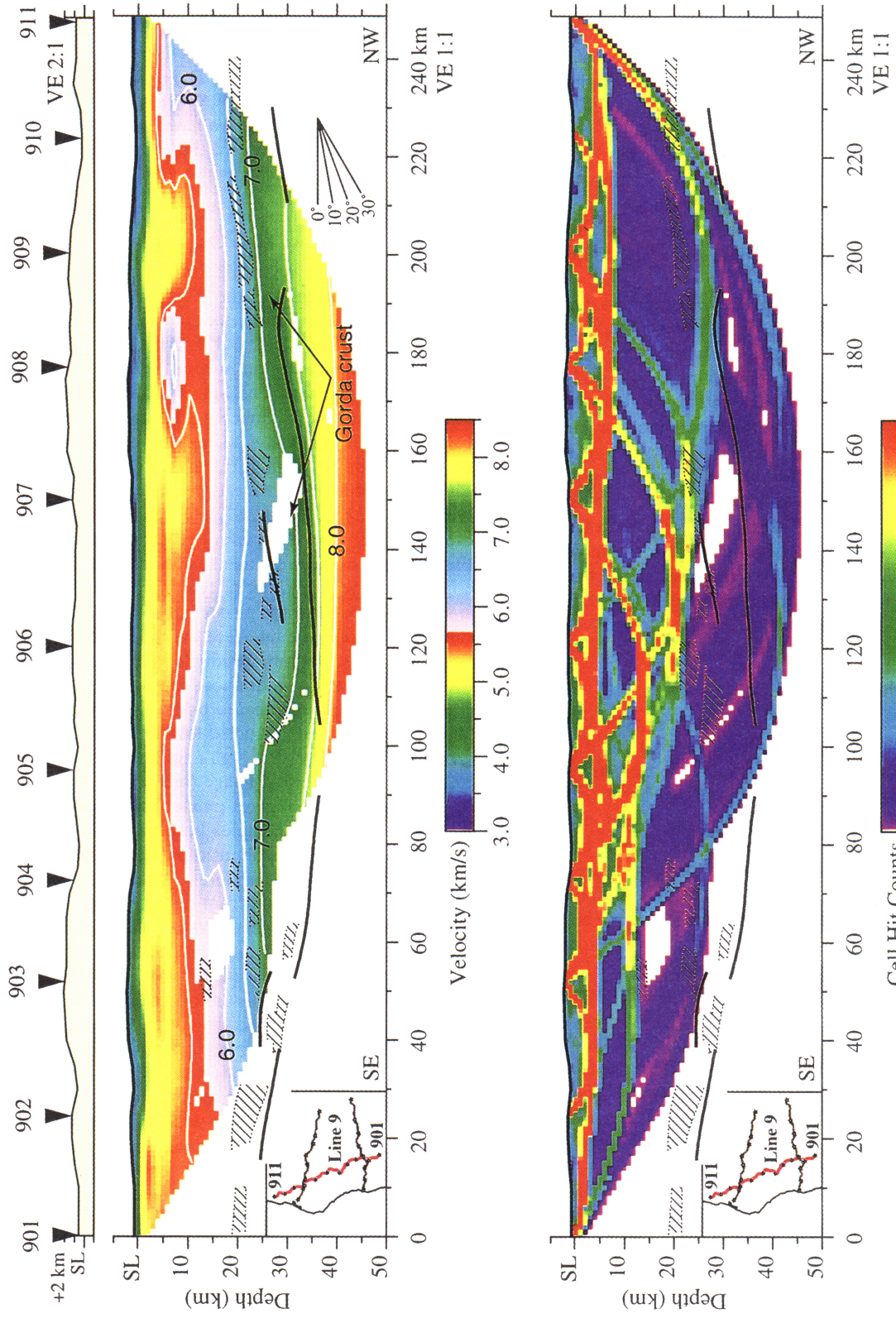

Plate 1. (top) Velocity model for line 9. Overlain on the model are reflectors based on both wide-angle reflections (heavy black lines) and regions of high-amplitude reflections from depth-migrated single-fold data (Figure 4) (hachured regions). White lines are velocity contours (km/s). The extent of the color image represents the extent of diving-ray coverage. Topography, vertically exaggerated by a factor of 2, and shot points 901 through 911 are shown above the model. (bottom) Color scale shows number of source-receiver rays passing through each 1 km × 1 km cell in our two-dimensional tomographic inversion.

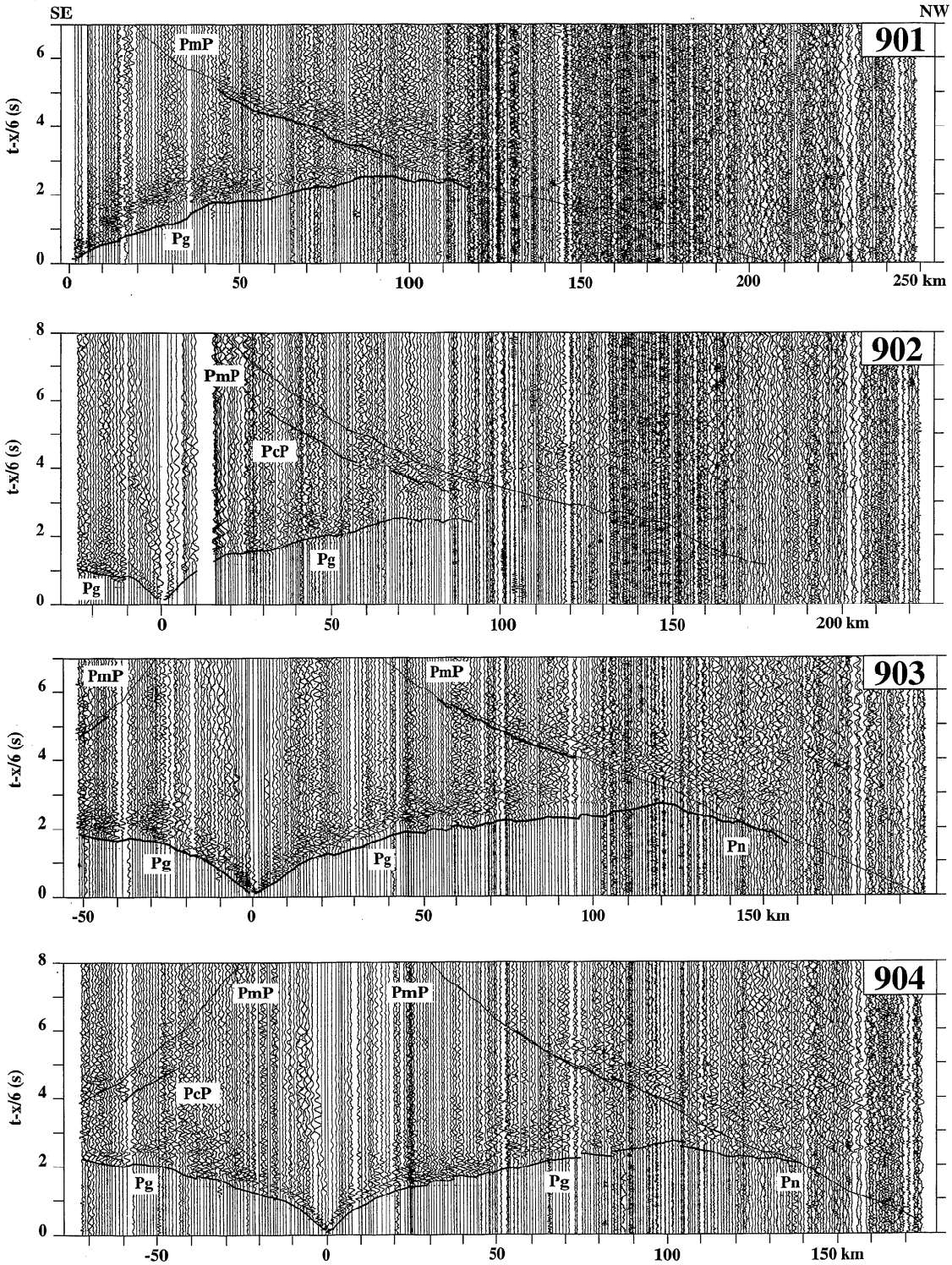

Figure 2. Record sections from line 9. Heavy black lines represent calculated travel times for all arrivals used in the velocity and interface inversion. Thin black lines represent calculated travel times for the gravity Moho (see text). Data are filtered from 2 to 16 Hz and trace normalized. Time is reduced by 6 km/s. *Pg*, crustal diving wave; *PcP*, reflections from the lower crustal layer; *PmP*, reflections from the Moho; *Pn*, mantle diving wave.

models this interface with an rms residual of ±0.31 km in depth (Figure 4a). Wide-angle reflections from the Gorda plate Moho are observed on shot points 904–911 (Figure 2). Both forward and inverse modeling position a dipping interface that is 35–36 km deep at model coordinate 100 km and shallows northwestward to 26–27 km at model coordinate 230 km. The inverse method models this interface with an rms residual of ±0.96 km in depth (Figure 4b).

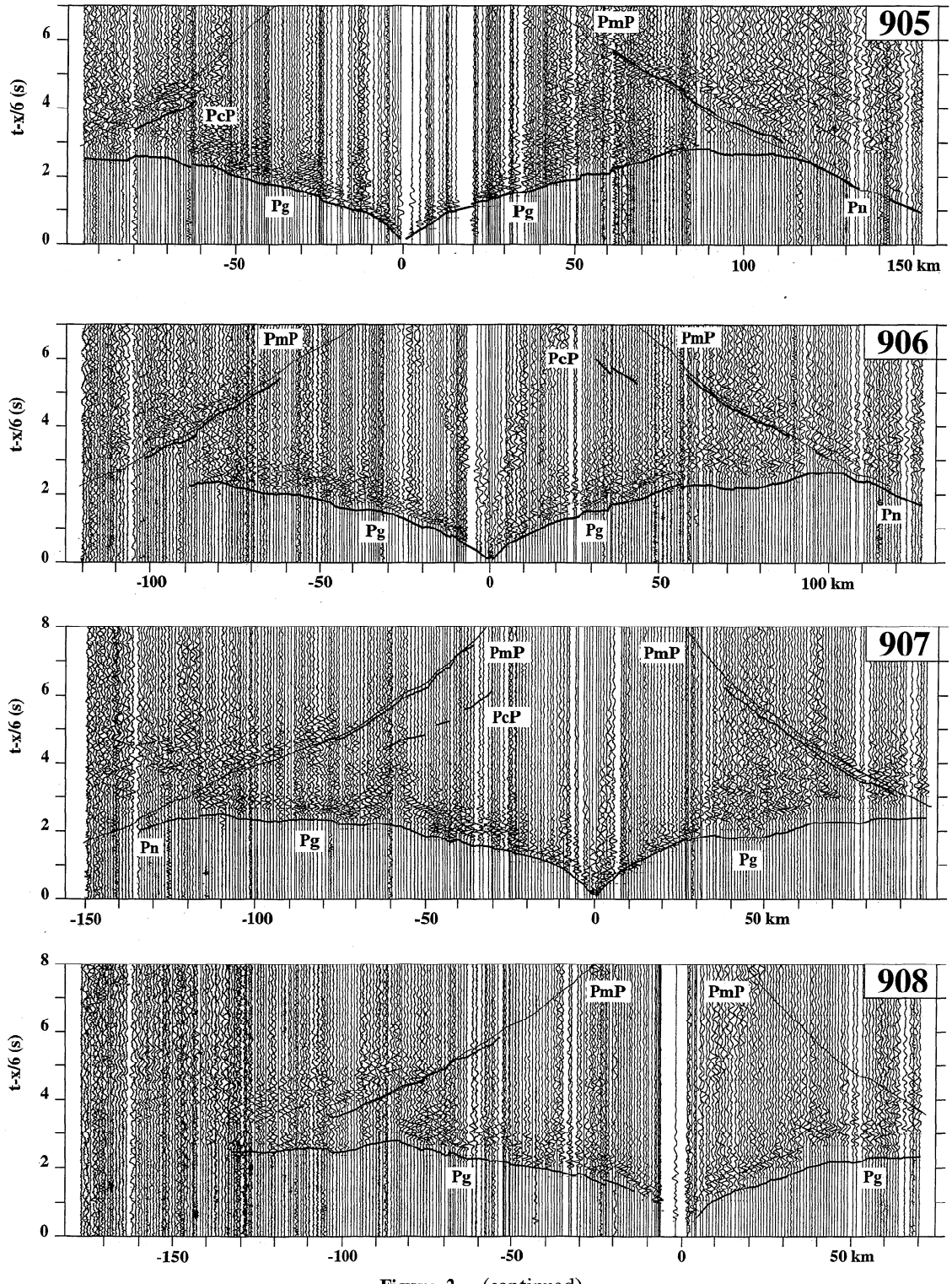

Figure 2. (continued)

3.1.2. The transform regime (model coordinates ~0–110 km). Crustal refracted arrivals from the transform regime define a laterally uniform Franciscan complex down to 20 km depth. This depth coincides with the 6.5 km/s contour as in our model for the subduction regime. Refracted arrivals from deeper in the model are confined to an arrival observed on shot points 901 and 907 that define a higher velocity, ~7.0–7.5 km/s, between model coordinates ~30–90 km. Absent from these data are *Pn* arrivals that sample the mantle south of model coordinate ~100 km (shot points 901 and 902 did not propagate to distances ≥140 km).

Basal crustal reflections from the depth-migrated single-fold data are grouped in two sets, a shallow set that roughly follows the 6.5 km/s contour and a gently NW dipping set that is ~5 km deeper (Plate 1 and Figure 3). Wide-angle reflections from shot points 901, 904, and 905 define a short reflector between

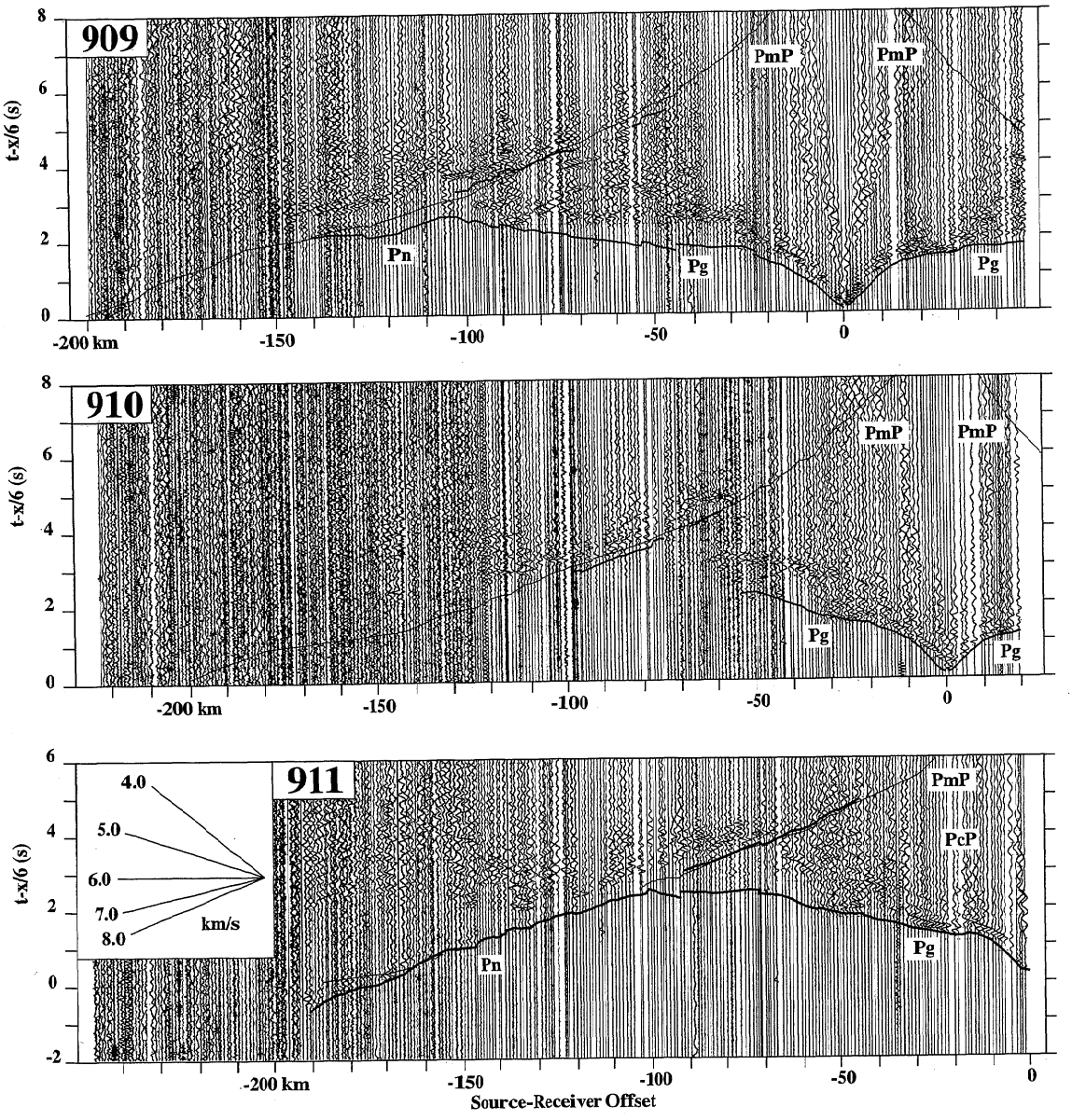

Figure 2. (continued)

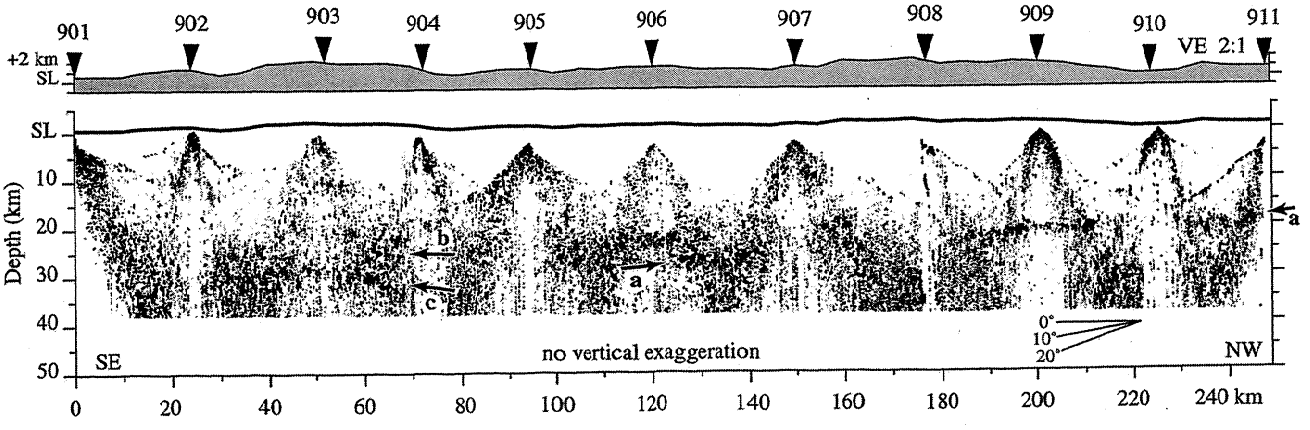

Figure 3. Depth-migrated single-fold image from precritical reflections at offset of ≤30 km; a arrows are reflections interpreted as top or near-top of Gorda crust, and b and c arrows are basal crustal reflections.

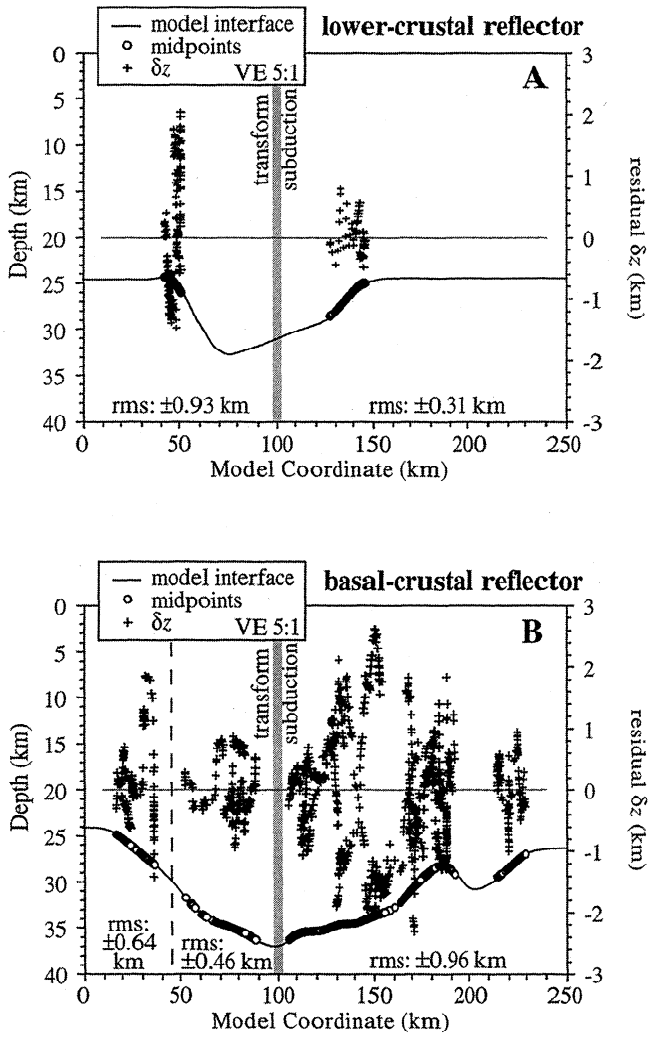

Figure 4. Splined interfaces for (top) lower crustal and (bottom) basal crustal reflectors (shown as heavy black lines in Plate 1), midpoints, and residuals for the interfaces modeled using the inversion technique.

model coordinates ~40–55 km that coincides with the shallower set of reflections from the depth-migrated single-fold section. This interface has an rms residual of ±0.93 km in depth (Figure 4a). Two deeper reflectors are modeled from the wide-angle reflections in this region of the transform regime. The first, sampled by shot points 901 and 903, is at a depth and a dip that agree with the single-fold data. This segment is modeled with an rms residual of ±0.64 km in depth (Figure 4b). The second segment, defined by shot points 903 and 906, dips gently to the NW, coincides with the single-fold data, and extends from model coordinate ~55–90 km. The inverse method models this segment with an rms residual of ±0.46 km in depth (Figure 4b). Ray coverage for this segment does not overlap with the deepest reflection north of model coordinate 100 km.

3.2. Constrained Gravity Modeling

Prior to collecting the MTJSE data, little was known about crustal structure in northern California. Existing data included unreversed seismic refraction data [*Warren*, 1981], seismic refraction data north of the MTJ [*Beaudoin et al.*, 1994], crustal tomography [*Verdonck and Zandt*, 1994], and mantle tomography [*Benz et al.*, 1992]. This restricted models of the gravity field to making broad assumptions based on these sparse data and observations of Benioff zone seismicity [e.g., *Jachens and Griscom*, 1983]. With our new seismic data we are able to refine the crustal structure used in these earlier models and hence to utilize the gravity data to further constrain various models of lower crustal/upper mantle geometry.

3.2.1. Jachens and Griscom model (Figure 7a). *Jachens and Griscom* [1983] modeled the isostatic residual gravity field along six profiles oblique to line 9 (Figure 5). Five of their profiles and our line 9 all sample a pronounced gravity low of ≥50 mGal below regional average. Lacking any control on crustal thickness Jachens and Griscom assumed a uniform North American (Franciscan) crustal thickness of 20 km (Plate 2a) above Gorda plate lithosphere to the north, and asthenosphere (slabless-window model) to the south. The essential components of their model are (1) a low-density tabular body (Gorda crust and mantle juxtaposed against asthenosphere to the south) creating a gravity decrease to the north; and (2) a wedge of higher density (relative to Franciscan) Klamath rocks on the northern end of their profiles to create a gravity increase at the northern end of the model. Their introduction of the Klamath terrane into the model was largely unconstrained at the time of their writing. Although the Jachens and Griscom assumption of constant crustal thickness has the merit of simplicity, here [*Beaudoin et al.*, 1996; *Godfrey et al.*, 1997; T. J. Henstock and A. Levander, Lithospheric evolution in the wake of the Mendocino Triple Junction: Structure of the San Andreas fault system at 2 Ma, submitted to *Journal of Geophysical Research*, 1998, hereinafter referred to as Henstock and Levander, submitted manuscript, 1998] as elsewhere in California [e.g., *Fuis and Mooney*, 1990] crustal thickness increases by 5–10 km from the coast to 100 km inland, rendering their conclusions invalid.

As seen in Plate 2a, Bouguer gravity along line 9 can be modeled incorrectly using a model similar to that of Jachens and Griscom (rms residual of 4.8 mGal). "Incorrect" because, unlike the profiles of Jachens and Griscom, line 9 does not cross any exposed Klamath rocks. Furthermore, the velocity field presents no indication of significant velocity differences, and hence inferred density differences, in the upper ~20 km of crust (Plate 1) [cf. *Beaudoin et al.*, 1996]. Without the Klamath body, this "Jachens and Griscom"-type model does not fit the observed Bouguer gravity (Plate 2a). We are therefore compelled to evaluate a suite of models, based on our velocity model, that vary only in lower crustal or upper mantle geometry in order to determine permissible plate geometry beneath line 9.

3.2.2. Gravity models derived from the velocity model. Below we discuss additional constraints that gravity modeling, based on our velocity model, offers to understanding lithospheric structure in the vicinity of the Mendocino Triple Junction and in particular along the southern edge of the Gorda slab. A smoothed version of our velocity model was converted to MacRay format for the gravity modeling [*Luetgert*, 1992]. Features in these density models that are held constant are the density structure of the Franciscan rocks above 20 km depth and the apparent dip of the Gorda plate. In all of these 2.5-D models, the thickness of Gorda lithosphere is based on a trench age of 5.3 Ma and a half spreading rate of 38 mm/yr for the last 5 Myr [*Riddihough*, 1984] giving an approximate age of 8 Ma and thickness of ~30–35 km for the lithosphere beneath

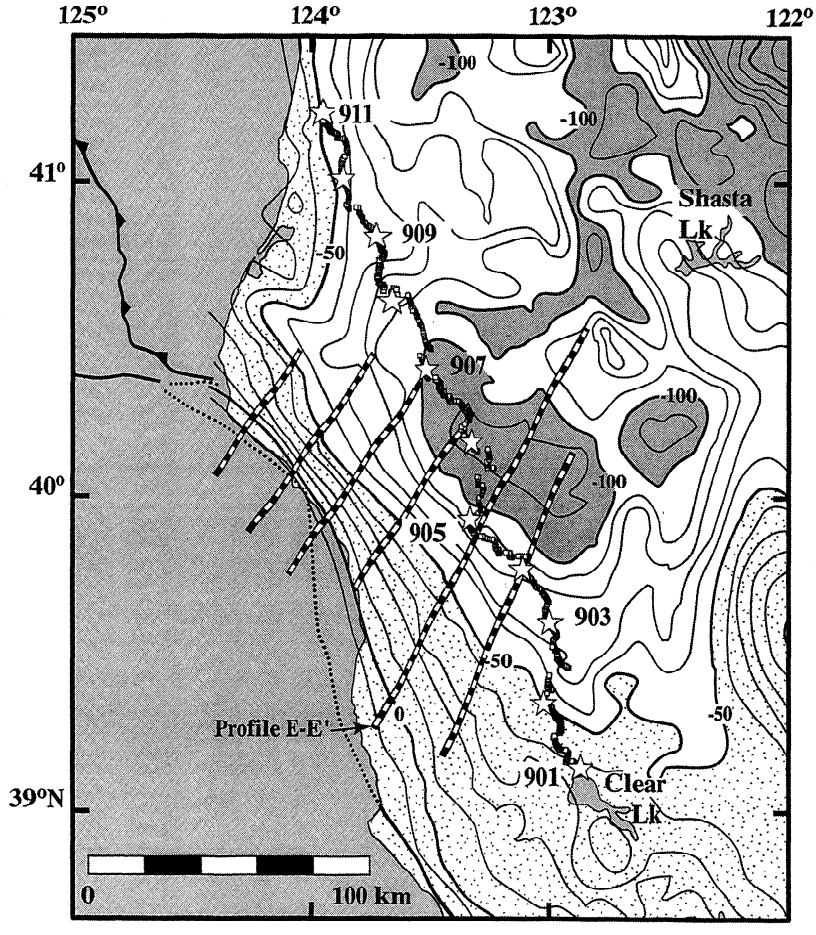

Figure 5. Bouguer gravity in the region of line 9 [after *Oliver et al.*, 1980]. Dashed lines represent profiles modeled by *Jachens and Griscom* [1983]. Shaded are regions of ≤ −100 mGal anomaly. Stipple is region of ≥ −50 mGal anomaly.

line 9. A density contrast of 0.04 g/cm^3 is used across the lithosphere-asthenosphere boundary.

3.2.2.1. Direct conversion (Plate 2b): Our first model is a direct conversion of the velocity model to density using a simple velocity-density conversion appropriate for Franciscan rocks [see *Godfrey et al.*, 1997, Figure 7) (Plate 2b). From this model it is evident that the apparent dip of the Gorda slab (corresponding to yellow and orange colors in Plate 2b) will provide much of the needed northward increasing Bouguer anomaly on the northern end of line 9. The large mismatch on the southern end indicates that further adjustment to the lower crust or upper mantle is required in this region. This model has an rms residual of 26.4 mGal.

3.2.2.2. Adjusted gravity Moho (Plate 2c): The first logical modification to our direct conversion model is to adjust the gravity Moho to coincide with the modeled reflector depths from the wide-angle reflections. This is justified because the tomographic inversion smoothes this contrast, as discussed above. A density discontinuity was therefore introduced to coincide with the basal crustal reflectors. With this change, the observed Bouguer anomaly is remarkably well matched (rms residual of 9.7 mGal), implying that most of the gravity anomaly can be accounted for by structure in the lower crust. The predicted anomaly is only weakly sensitive to the variations in mantle geometry if the mantle density remains constant along the profile.

3.2.2.3. Preferred model (Plate 2d): Finally, we introduce a lateral change in upper mantle density as predicted by the slab window model. The lack of *Pn* arrivals from shot points 901 and 902 (Figure 2) and the extent of modeled ray coverage (see Plate 1) suggest a zone of increased scattering, intrinsic attenuation, or both that affects energy propagation through the center of our model [cf. *Beaudoin et al.*, 1996]. We attribute this zone of attenuation to the southern edge of the Gorda slab (SEDGE). With this in mind, our preferred model introduces a slab edge (SEDGE) that coincides with the envelope of ray coverage (Plate 1; dashed white line, Plate 2). By introducing this 3.20–3.23 g/cm^3 tabular body on the northern end, we are required also to include a sub-Moho 3.20–3.23 g/cm^3 high-density wedge on the southern end of the profile to fit the observed gravity. The boundary between Gorda crust and the southern basal crustal layer was also adjusted from model coordinate 110 km to 95 km to better fit the gravity low in the center of the profile. The final model has an rms residual of 5.8 mGal with the largest misfits between model coordinates 90–130 km. Removing either the high-density wedge at Moho depths on the southern end or the Gorda mantle slab on the northern end degrades the fit (rms residuals of 11.7 mGal rms and 20.0 mGal rms, respectively, Plate 2d).

Our preferred model has four main features: (1) The North American crust is thickest in the center of the profile. This thickening of low-density rocks in the middle of the profile is

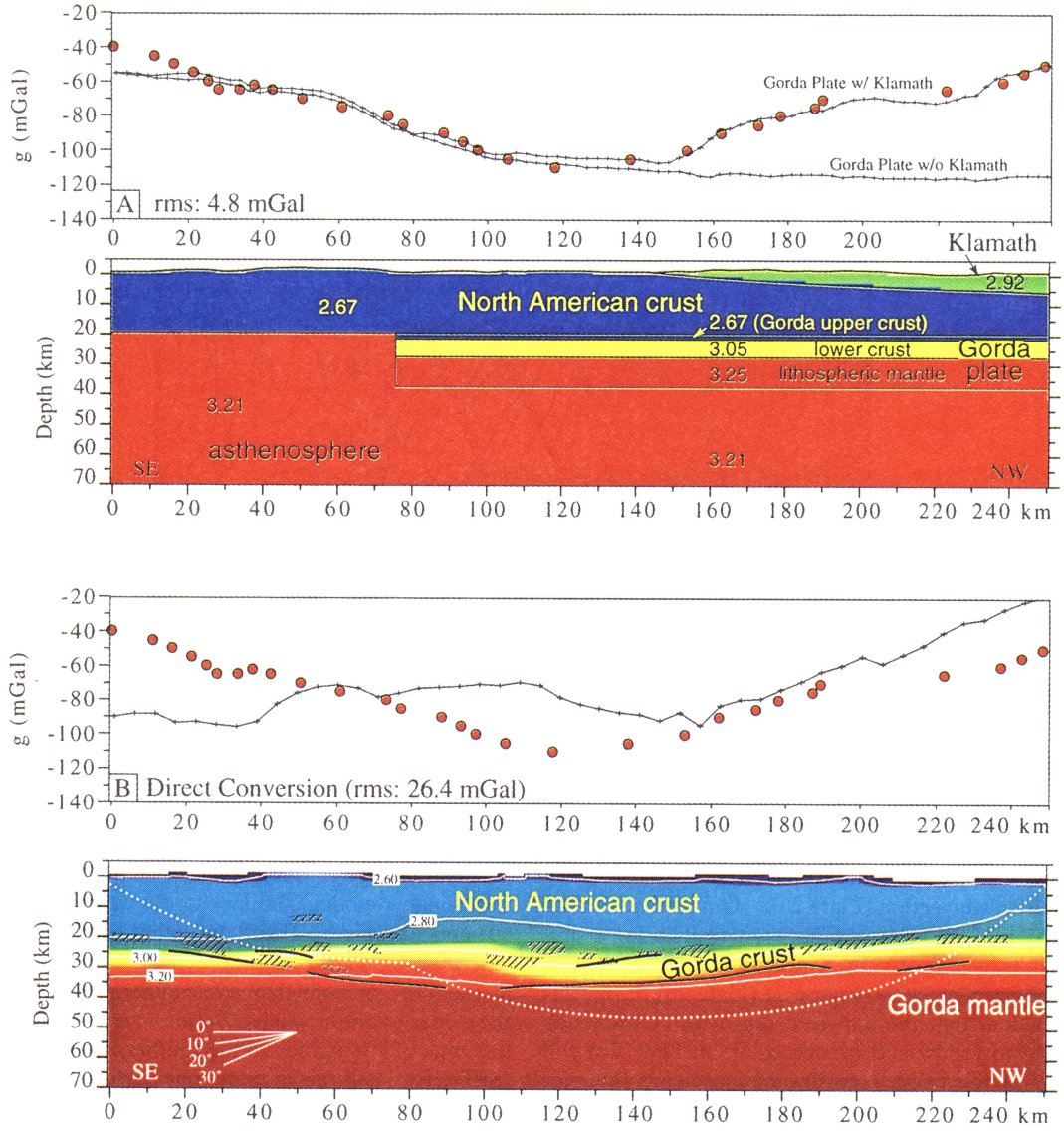

Plate 2. Gravity models along line 9. Dotted white line, the ray coverage of our velocity model (see Figure 2). Solid white lines, density contours. Red circles, the observed Bouguer gravity along line 9. (a) *Jachens and Griscom* [1983] model (profile E-E′ in Figure 5) rotated and modified to fit the Bouguer gravity along line 9. (b) A direct conversion of the velocity model to density. (c) Same as Plate 2b with the Moho adjusted to match basal crustal reflectors. (d) The best fit model with changes made to densities only beneath 20 km depth. Also shown are the effects of removing the Gorda lithospheric mantle on the north and postulated lithospheric mantle wedge on the south. (e) Variations in location of southern edge of Gorda slab.

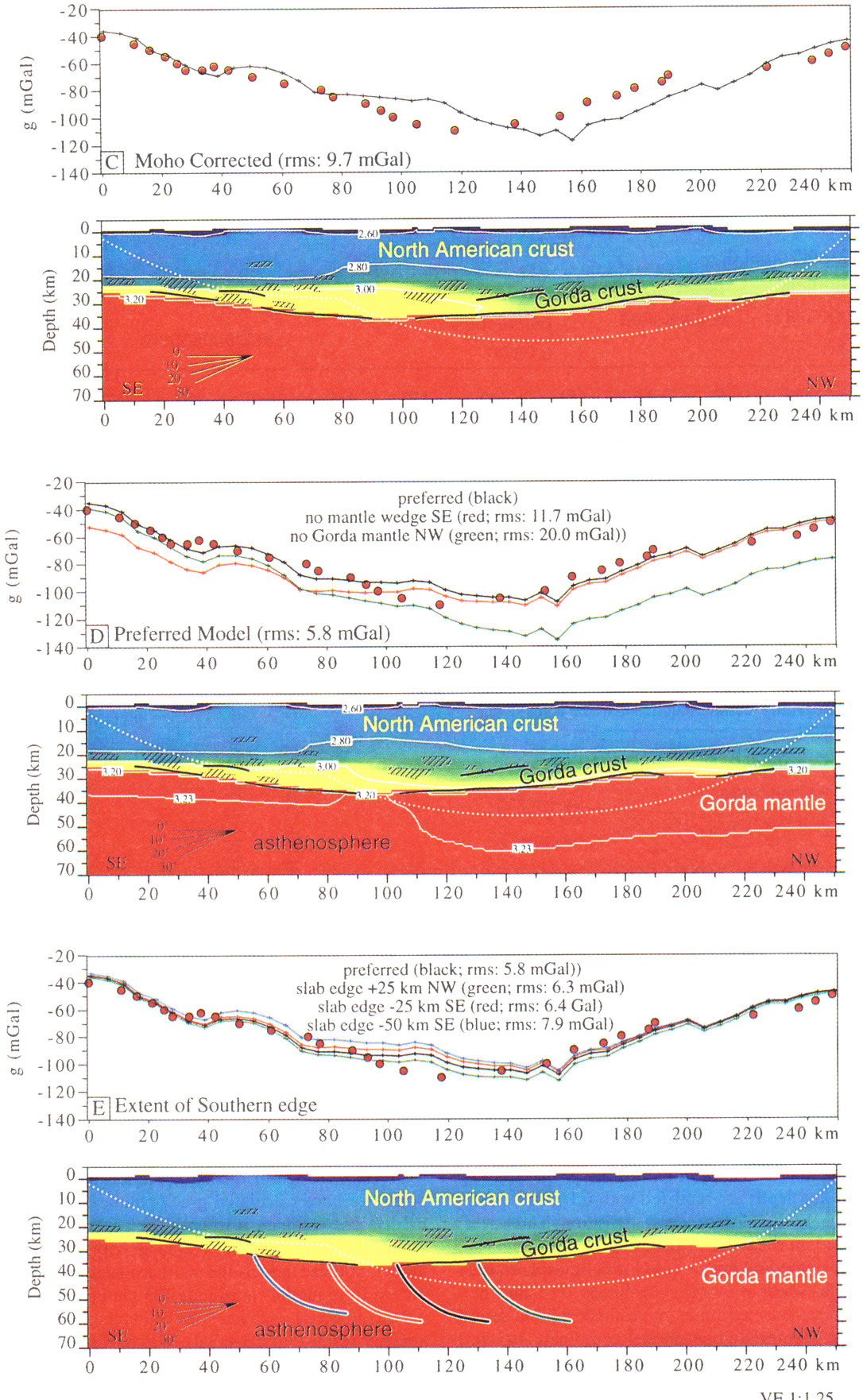

Plate 2. continued

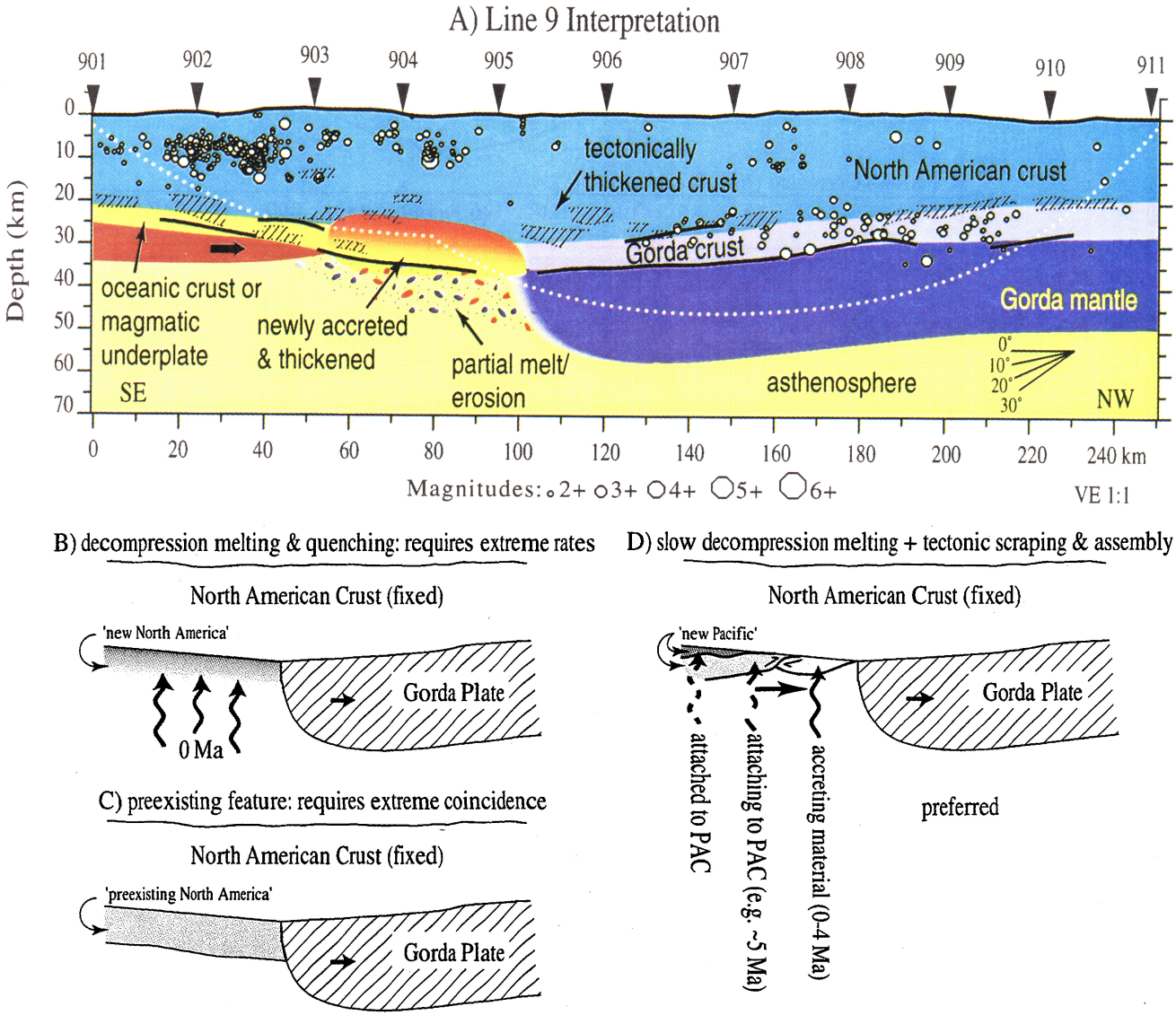

Plate 3. (a) Interpretation of our velocity model. Overlain are interfaces determined from wide-angle reflections (heavy black lines), regions of high reflectivity from the depth-migrated single-fold image (hachured), velocity model ray coverage (dotted white line), and hypocenters for 1984–1994 from the Northern California Seismic Network catalog within 7.5 km of the profile (octagons, hypocenters have errors in depth of ≤2.5 km and lateral position of ≤1.5 km). Below are three possible explanations for the body of mafic material at the base of North American crust and immediately adjacent to the Gorda slab. (b) Decompression melting and rapid quenching adding material to the North American plate. (c) A preexisting feature of the North American plate. (d) Slow decompression melting coupled with tectonic off-scraping and assembly of the basal crustal material as part of the Pacific plate.

based on the well-sampled, low velocities observed in the inverse model. (2) On the southern end of the profile the high velocities at 23 km depth are modeled with 0.1 g/cm^3 density increase relative to the Gorda crust densities. This layer's thickness is based on reflections from both the wide-angle and depth-migrated single-fold image. (3) Gorda lithosphere is extended only as far south as model coordinate ~110 km where mantle lithosphere densities grade into asthenospheric density over 10 km (e.g., centered about model coordinate 105 km). (4) A high-density wedge is present at Moho depths beneath the southern end of our profile. However, the thickness of this wedge is poorly determined.

3.2.2.4. Southern edge of the Gorda slab (Plate 2e). In this final model we test the sensitivity of our preferred model to the location of the southern edge of the Gorda plate (SEDGE). Using our preferred model (Plate 2d) as a starting point, we have calculated gravity along our profile for three models and compare it to both the observed Bouguer gravity along line 9 and the calculated gravity from our preferred model. In these models the southern edge of the Gorda slab is moved from model coordinate 105 km by −50 km (rms residual of 7.9 mGal), −25 km (rms residual of 6.4 mGal), and +25 km (rms residual of 6.3 mGal). We conclude that our preferred location of SEDGE could be in error by ±25 km but that a shift of 50 km is precluded by our modelling.

In summary, first-order features from the velocity model that we demonstrate are needed to fit gravity data are the thickening of the overlying Franciscan terrane near the center

of our profile, the existence of a higher-density (relative to overlying Franciscan) lower crustal layer on the southern end of our profile, and the truncation of the Gorda plate near the center of our profile. Furthermore, given these features constrained by our seismic study, the gravity model requires the presence of high-density material below the Moho on the southern end of our profile.

Discussion

Travel time tomography using first arrivals along line 9 produces a model of relatively uniform velocity (<6.5 km/s) crust to depths of ~20 km (Plate 1). We interpret these velocities to indicate that Franciscan rocks extend to at least 20 km beneath our profile [*Thompson and Talwani*, 1964]. At depths greater than 20 km, south-to-north variations in both the velocity field and model ray penetration are observed. In our "transform regime" between shot points 903 and 905, high velocities (7.0–7.5 km/s) occur at 23 km depth. A similar onset of higher velocities (an increase from ~6.5 to 7.0 km/s) is modeled along crossing profile line 1 [*Godfrey et al.*, 1997; Henstock and Levander, submitted manuscript, 1998]. Dip on this "layer" is poorly constrained. In our "subduction regime" from shot points 906 to 910, velocities >7.0 km/s define a southward dipping zone from 22 km depth beneath shot point 910 to 28 km depth beneath shot point 906.

Within the North American crust, line 9 indicates a deepening (~10 km) of the 7.0 km/s velocity contour in the center of our profile. A similar result, interpreted as thickened North American crust along the eastward projection of the Mendocino fracture zone, has recently been reported by *Verdonck and Zandt* [1994]. Verdonck and Zandt interpret their model to indicate that the Gorda slab is flexing downward 6–12° to the south and that the local thickening of the North American crust is either due to compressional forces associated with Pacific plate convergence or underthrusting of the accretionary complex along the Cascadia Subduction Zone. Our line 9 model is only 10° oblique to the local trend of the Cascadia Subduction Zone, and therefore we expect no more than half of the crustal thickening to be attributed to moving downdip, southward along our profile (~4–5 km depth variation between shot points 911 and 906 for a 10° obliquity and a 12° dip on the Gorda slab). If, however, the Gorda slab is flexing southward as suggested by Verdonck and Zandt, our data suggest a maximum of 5° southward flexing. We prefer to interpret the overthickened North American crust as tectonic thickening in response to the northward convergence between Pacific and Gorda plates rather than underthrust accretionary complex [*Beaudoin et al.*, 1996; *Tréhu et al.*, 1995] because we are forced (Plate 3) to adopt a similar tectonic thickening model to explain our uppermost mantle observations.

Reflections from the lower crust and Moho are observed in both the wide-angle and depth-migrated single-fold data (Plate 1 and Figure 3). North of shot point 905, a south dipping zone of high-velocity material is coincident with south dipping reflectors interpreted as Gorda plate Moho. The high-amplitude reflections above Gorda plate Moho (arrows on Figure 3) are interpreted to originate at or near the North American–Gorda plate boundary. This interpretation is consistent with models for MTJSE line 6 [*Beaudoin et al.*, 1996; *A. M. Tréhu et al.*, manuscript in preparation, 1998], earthquake hypocenters, and projected Gorda slab depth [cf. *Beaudoin et al.*, 1994]. Utilizing both the wide-angle reflection modeling and the depth-migrated single-fold section, we can trace the Gorda crust reflections from shot point 911 to just south of shot point 907, coincident with the termination of Gorda slab seismicity (Plate 3a). At this point we are unable to determine whether the reflectivity beneath shot point 906 is genetically associated with the reflective band to the north or with the more diffuse but locally strong, reflectivity to the south. However, based on first-arrival ray coverage and the wide-angle reflections, Gorda Moho extends beyond these Gorda crust reflections to between shot points 905 and 906 (Plate 3a). Finite difference modeling of amplitudes of *Pn* and *PmP* on shot point 911 supports this interpretation [*Lendl*, 1996].

We interpret the deep structure beneath line 9 determined from seismic and gravity data to indicate that the southern edge of the Gorda slab is between shot points 905 and 906 (Plate 3a). Changes in Gorda crust reflectivity and cessation of slab-associated seismicity ~30 km north of this edge may be due to either changes in slab continuity or a change in lithologies and therefore impedance contrast and coupling, across the North American–Gorda plate boundary. On the basis of our velocity and gravity modeling our model is generally compatible with that of *Jachens and Griscom* [1983], in which the Gorda slab extends as far south as approximately shot point 904, although our preferred model places the southern edge about 25 km farther north.

The lower crust/upper mantle reflectivity and velocity structure observed near the southern end of line 9 is consistent with that modeled for line 1, which intersects our profile north of shot point 902 (Plate 1) [*Godfrey et al.*, 1997; *Levander et al.*, 1998; Henstock and Levander, submitted manuscript, 1998]. The ~5 km of mafic material (6.5 km/s $\leq V_p \leq$ 7.5 km/s) overlying mantle can be interpreted as either tectonically underplated oceanic crust [cf. *Benz et al.*, 1992] or magmatically accreted mafic material [cf. *Furlong et al.*, 1989]. We cannot distinguish between these two models on the basis of velocity alone.

The modeled shallow (~23 km) high velocities and densities in the center of our profile suggest up to 10 km of mafic material exists at the base of the North American crust immediately adjacent to the southern edge of the Gorda slab. Here we explore three possible explanations for this body of mafic material. The first explanation is a localized region of basal underplating (Plate 3b). Thermomechanical modeling indicates that in ~5 m.y. 5–10 km of basaltic underplate could be generated after passage of the MTJ by decompression melting of the rising asthenosphere [*Furlong and Fountain*, 1986; *Liu and Furlong*, 1992]. However, for decompression melting to be the mechanism creating this layer requires that we invoke maximum decompression melting, complete melt segregation, and nearly instantaneous quenching to produce the structure observed, i.e., conditions that seem unlikely. A second explanation is that this body is a preexisting structure of unknown origin (Plate 3c), which also seems unlikely since we see no evidence for similar lower crustal structure north of this region. It seems an unlikely coincidence that such a preexisting feature would coincide with the southern edge of the Gorda slab today, rather than arbitrarily in the past or future. Our preferred explanation is a model whereby basal underplating is occurring at expected rates but at a lower rate than required to create the entire thickness of mafic material modeled here (Plate 3d). As this new material cools, it is accreted to the eastern edge of the Pacific plate [cf. *Furlong et al.*, 1989] and moves northward with respect to North America. With this northward movement the

leading edge of this "new Pacific" begins to scrape off additional material from the base of North America. In this manner, the mafic body is constructed by both magmatic underplating and tectonic thickening. Although this model can explain observations along our profile, inconsistencies exist when comparing to observations from other wide-angle seismic profiles [*Hole et al.*, 1998]. Most notable is evidence from onshore/offshore line 1 that suggests the southern basal crustal layer, like the overlying North American crust, is faulted and therefore most likely part of the North American crust [*Henstock et al.*, 1997]. This requires that the basal layer be coupled to the North American plate and hence unable to move northward to act as a bulldozer off-scraping material along its leading edge.

In our model (Plate 3a) the lithospheric mantle is thinnest just south of the southern edge of the Gorda plate and increases in thickness to produce a wedge to the south. This geometry is consistent with a model in which the asthenosphere rises to the base of the crust in a slabless window created by the northward movement of the Gorda plate and then cools, creating magmatic underplating and new mantle lithosphere, as a function of time since passage of the triple junction. Our proposed model for the thickening of the lower crustal mafic layer overlying the region of thin mantle lithosphere implies that this mantle lithosphere and the overlying mafic crust are welded to the Pacific plate and move north with it relative to North America. This result supports the offset-plate-boundary model, as developed by *Furlong et al.* [1989], rather than the model of *Bohannon and Parsons* [1995] which predicts significantly older, and therefore thicker, lithosphere adjacent to the subducted Gorda slab.

South of our interpreted SEDGE, the region of thickened Franciscan complex and basal underplating overlies a zone of increased scattering, intrinsic attenuation, or both, resulting from mechanical mixing of lithologies and/or partial melt left in the wake of the Gorda plate. Our model suggests that there is newly accreted material at the base of the Franciscan rocks, perhaps coupled with alteration of the lower crust or assimilation into melt triggered by upwelling asthenosphere [e.g., *Johnson and O'Neil*, 1984; *Liu and Furlong*, 1992]. This newly accreted material is at least localized along the southern edge of the Gorda slab and may extend southward to the end of our profile. Melts penetrating up into the crust, or lower crustal fluids released during prograde metamorphism of overlying North America, give rise to seismic bright spots below shot point 903 [cf. *Levander et al.*, 1998].

4. Conclusions

The MTJSE provides new seismic data that image changes in crustal and uppermost mantle structure associated with the passage of the Mendocino Triple Junction. The crustal velocity model shows, on average, a laterally homogeneous velocity for the Franciscan terrane and the greatest thickness of $\leq$7.0 km/s lithologies in the center of our profile. The high densities and velocities at 23 km depth in the center of our profile are interpreted as newly accreted material at the base of the Franciscan rocks, perhaps coupled with alteration of the lower crust or assimilation into melt triggered by upwelling asthenosphere. This newly accreted material has been tectonically thickened in response to either underthrust oceanic crust or newly accreted material that is coupled to the Pacific plate and is therefore moving north relative to the overlying North American plate.

Important in our observations and interpretation are the variations of lower crustal reflectors along line 9 and the thickening of mantle lithosphere to the south. The variations in lower crustal reflectors and the apparent absorption of seismic energy from the southern shots support a zone of increased scattering, intrinsic attenuation, or both, resulting from mechanical mixing of lithologies and/or partial melt in the central region of line 9 beneath the onshore projection of the Mendocino fracture zone. This zone of attenuation combined with the southward thickening mantle lithosphere indicates that our profile crosses the southern edge of the Gorda plate and that directly adjacent to this edge is an asthenospheric window.

Acknowledgments. Supported by National Science Foundation grants EAR-9218209, EAR-9219870, EAR-9218968, and EAR-9219598 and by the U.S. Geological Survey Deep Continental Studies program. Volunteers from Stanford, Rice, Oregon State, Lehigh, and Humboldt State Universities and the U.S. Geological Survey were crucial to the success of this project. We particularly thank Ed Criley and the Crustal Studies Group at the USGS. Seismographs from the Program for Array Seismic Studies of the Continental Lithosphere (PASSCAL), Stanford University, and the Geological Survey of Canada were used in this research. Land use, graciously permitted by individuals, corporations, and government, was essential to our success. Specifically, we would like to thank Bob Bremner, Craig Brown, Lee Bucknell, David Dodd, Bill Feeney, Gilbert Martin, Michael Ward, Anderson Solid Waste (Rick Morton), Bureau of Land Management (Michael Truden), Circle X Ranch (Marilyn Brooks), Georgia Pacific Co. (Tom Ray), Hoff Trust (Marie Hoff), Louisiana Pacific Co. (Dave Shantz and Roger Krueger), Mendocino National Forest (David Roak), Pacific Lumber Co. (Tom Herman), Redwood National Park Service (Edward Haberlin), Sierra Pacific Industries (Jack Frost), Simpson Timber Co. (Juergen Momber), Six Rivers National Forest (Meredith Smith), Soper-Wheeler Co. (James Soper), and Stover Ranch (Libby George). For use of their facilities during our field operation we extend thanks to Humboldt State University and Blosser Lane Elementary School (Charles Davison).

References

Atwater, T., Implications of plate tectonics for the Cenozoic tectonic evolution of western North America, *Geol. Soc. Am. Bull.*, *81*, 3513–3536, 1970.

Beaudoin, B. C., M. Magee, and H. Benz, Crustal velocity structure north of the Mendocino Triple Junction, *Geophys. Res. Lett.*, *21*(21), 2319–2322, 1994.

Beaudoin, B. C., et al., The transition from slab to slabless: Results from the 1993 Mendocino Triple Junction Seismic Experiment, *Geology*, *24*, 195–199, 1996.

Benz, H. M., G. Zandt, and D. H. Oppenheimer, Lithospheric structure of northern California from teleseismic images of the upper mantle, *J. Geophys. Res.*, *97*, 4791–4807, 1992.

Blake, M. C., Jr., and A. S. Jayko, Tectonic evolution of northwest California and southwest Oregon, *Bull. Soc. Geol. Fr.*, *6*, 921–930, 1986.

Blake, M. C., Jr., A. S. Jayko, and R. J. McLaughlin, Tectonostratigraphic terranes of the northern Coast Ranges, California, in *Tectonostratigraphic Terranes of the Circum-Pacific Region*, edited by D. G. Howell, pp. 159–186, Circum-Pac. Counc. for Energy and Miner. Resour., Houston, Tex., 1985.

Bohannon, R. G., and T. Parsons, Tectonic implications of post-30 Ma Pacific and North American relative plate motions, *Geol. Soc. Am. Bull.*, *107*, 937–959, 1995.

Brocher, T. M., J. McCarthy, P. E. Hart, W. S. Holbrook, K. P. Furlong, T. V. McEvilly, J. A. Hole, and S. L. Klemperer, Seismic evidence for a lower-crustal detachment beneath San Francisco Bay, California, *Science*, *265*, 1436–1439, 1994.

Carver, G., and R. B. Burke, Active convergent tectonics in northwestern California, in *Geologic Evolution of the Northernmost Coast Ranges and Western Klamath Mountains*, California, *Field Trip Guide.*, vol. T308, edited by K. R. Aalto and G. D. Harper, pp. 64–82, AGU, Washington, D. C., 1989.

Castillo, D. A., and W. L. Ellsworth, Seismotectonics of the San Andreas fault system between Point Arena and Cape Mendocino in northern California: Implications for the development and evolution of a young transform, *J. Geophys. Res.*, *98*, 6543–6560, 1993.

Clarke, S. H., Jr., Geology of the Eel River basin and adjacent region: Implications for late Cenozoic tectonics of the southern Cascadia subduction zone and Mendocino Triple Junction, *AAPG Bull.*, *76*, 199–224, 1992.

Clarke, S. H., Jr., and G. A. Carver, Late Holocene tectonics and paleoseismicity, southern Cascadia subduction zone, *Science*, *255*, 188–192, 1992.

Dickinson, W. R., Plate tectonics and the continental margin of California, in *The Geotectonic Development of California*, edited by W. G. Ernst, pp. 1–28, Prentice-Hall, Englewood Cliffs, N. J., 1981.

Dickinson, W. R., and W. S. Snyder, Geometry of triple junctions related to San Andreas transform, *J. Geophys. Res.*, *84*, 561–572, 1979.

Fox, K. F., Jr., R. J. Fleck, G. H. Curtis, and C. E. Meyer, Implications of the northwestwardly younger age of volcanic rocks in west-central California, *Geol. Soc. Am. Bull.*, *96*, 647–654, 1985.

Fuis, G. S., and W. D. Mooney, Lithospheric structure and tectonics from seismic-refraction and other data, in *The San Andreas Fault System, California, U.S. Geol. Surv. Prof. Pap.*, *1515*, 207–236, 1990.

Furlong, K. P., Lithospheric behavior with triple junction migration: An example based on the Mendocino Triple Junction, *Phys. Earth Planet. Inter.*, *36*(3–4), 213–223, 1984.

Furlong, K. P., and D. M. Fountain, Continental crustal underplating: Thermal considerations and seismic-petrologic consequences, *J. Geophys. Res.*, *91*, 8285–8294, 1986.

Furlong, K. P., W. D. Hugo, and G. Zandt, Geometry and evolution of the San Andreas fault zone in northern California, *J. Geophys. Res.*, *94*, 3100–3110, 1989.

Godfrey, N. J., B. C. Beaudoin, C. Lendl, J. H. Luetgert, and A. S. Meltzer, Data report for the 1993 Mendocino Triple Junction Seismic Experiment, *U.S. Geol. Surv. Open File Rep.*, *95-0275*, 83 pp., 1995.

Godfrey, N. J., B. C. Beaudoin, and S. L. Klemperer, and the Mendocino Working Group, Ophiolitic basement to the Great Valley forearc basin, California, from seismic and gravity data: Implications for crustal growth at the North American continental margin, *Geol. Soc. Am. Bull.*, *109*, 1536–1562, 1997.

Griscom, A., and R. C. Jachens, Tectonic history of the north portion of the San Andreas fault system, California, inferred from gravity and magnetic anomalies, *J. Geophys. Res.*, *94*, 3089–3099, 1989.

Harper, G. D., The Josephine Ophiolite: Remains of a Late Jurassic marginal basin in northwestern California, *Geology*, *8*(7), 333–337, 1980.

Heaton, T. H., and S. H. Hartzell, Earthquake hazards on the Cascadia subduction zone, *Science*, *236*, 162–168, 1987.

Henstock, T. J., A. L. Levander, and J. A. Hole, Deformation in the lower crust of the San Andreas fault system in northern California, *Science*, *278*, 650–653, 1997.

Hole, J. A., Nonlinear high-resolution three-dimensional seismic travel time tomography, *J. Geophys. Res.*, *97*, 6553–6562, 1992.

Hole, J. A., and B. C. Zelt, 3-D finite-difference reflection traveltimes, *Geophys. J. Int.*, *121*, 427–434, 1995.

Hole, J. A., B. C. Beaudoin, and T. J. Henstock, Wide-angle seismic constraints on the evolution of the deep San Andreas plate boundary by Mendocino Triple Junction migration, *Tectonics*, *17*, 802–818, 1998.

Jachens, R. C., and A. Griscom, Three-dimensional geometry of the Gorda plate beneath northern California, *J. Geophys. Res.*, *88*, 9375–9392, 1983.

Johnson, C. M., and J. R. O'Neil, Triple junction magmatism: A geochemical study of Neogene volcanic rocks in western California, *Earth Planet Sci. Lett.*, *71*(2), 241–263, 1984.

Lachenbruch, A. H., and J. H. Sass, Heat flow and energetics of the San Andreas fault zone, *J. Geophys. Res.*, *85*, 6185–6222, 1980.

Lendl, C., Finite difference wavefield modeling of large-aperture data from the 1993 Mendocino Triple Junction Seismic Experiment, Master thesis, Oreg. State Univ., Corvallis, 1996.

Lendl, C., A. Tréhu, J. Goff, A. Levander, and B. Beaudoin, Synthetic seismograms through synthetic Franciscan: Insights into factors affecting large aperture data, *Geophys. Res. Lett.*, *24*, 3317–3320, 1997.

Levander, A. R., and R. L. Kovach, Shear velocity structure of the northern California lithosphere, *J. Geophys. Res.*, *95*, 19,773–19,784, 1990.

Levander, A., T. J. Henstock, A. S. Meltzer, A. M. Tréhu, B. C. Beaudoin, and S. L. Klemperer, A window through the lithosphere: Seismic images of active magmatic crustal accretion, *Geology*, *26*, 171–174, 1998.

Liu, M., and K. P. Furlong, Cenozoic volcanism in the California Coast Ranges: Numerical solutions, *J. Geophys. Res.*, *97*, 4921–4951, 1992.

Luetgert, J. H., Interactive seismic raytracing for the Macintosh™, *U.S. Geol. Surv. Open File Rep.*, *92-356*, 1992.

Oliver, H. W., R. H. Chapman, S. Biehler, S. L. Robbins, W. F. Hanna, A. Griscom, L. A. Beyer, and E. A. Silver, Gravity map of California and its continental margin, Calif. Div. of Mines and Geol., Sacramento, 1980.

Oppenheimer, D., et al., The Cape Mendocino, California, earthquakes of April 1992: Subduction at the triple junction, *Science*, *261*, 433–438, 1993.

Riddihough, R. R., Recent movements of the Juan de Fuca plate system, *J. Geophys. Res.*, *89*, 6980–6994, 1984.

Severinghaus, J., and T. Atwater, Cenozoic geometry and thermal state of the subducting slabs beneath western North America, in *Basin and Range Extensional Tectonics Near the Latitude of Las Vegas, Nevada*, edited by B. P. Wernicke, pp. 1–22, Geol. Soc. of Am., Boulder, Colo., 1990.

Thompson, G. A., and M. Talwani, Crustal structure from Pacific Basin to central Nevada, *J. Geophys. Res.*, *69*, 4813–4837, 1964.

Tréhu, A. M., and the Mendocino Working Group, Pulling the rug out from under California: Seismic images of the Mendocino Triple Junction region, *Eos Trans. AGU*, *76*(38), 369, 380–381, 1995.

Verdonck, D., and G. Zandt, Three-dimensional crustal structure of the Mendocino Triple Junction region from local earthquake travel times, *J. Geophys. Res.*, *99*, 23,843–23,858, 1994.

Warren, D. H., Seismic-refraction measurements of crustal structure near Santa Rosa and Ukiah, California, in *Research in the Geyser-Clear Lake Geothermal Area, Northern California*, edited by R. J. McLaughlin and J. M. Donnelly-Nolan, *U.S. Geol. Surv. Prof. Pap. 1141*, 167–182, 1981.

Wilson, D. S., A kinematic model for the Gorda deformation zone as a diffuse southern boundary of the Juan de Fuca plate, *J. Geophys. Res.*, *91*, 10,259–10,269, 1986.

Wilson, D. S., Deformation of the so-called Gorda plate, *J. Geophys. Res.*, *94*, 3065–3075, 1989.

Zandt, G., Seismic images of the deep structure of the San Andreas fault system, central Coast Ranges, California, *J. Geophys. Res.*, *86*, 5039–5052, 1981.

Zandt, G., and K. P. Furlong, Evolution and thickness of the lithosphere beneath coastal California, *Geology*, *10*, 376–381, 1982.

B. C. Beaudoin and S. L. Klemperer, Department of Geophysics, Stanford University, Mitchell Building, Stanford, CA 94305-2215. (e-mail: bruce@geo.stanford.edu)

J. A. Hole, Department of Geological Sciences, Virginia Tech, Blacksburg, VA 24061-0402. (e-mail: hole@vt.edu)

A. M. Trehu, College of Ocean and Atmospheric Sciences, Oregon State University, Corvallis, OR 97331.

(Received August 11, 1997; revised June 18, 1998; accepted June 19, 1998.)